

## RADIO PULSAR DEATH LINE REVISITED: IS PSR J2144-3933 ANOMALOUS?

BING ZHANG<sup>1,2</sup>, ALICE K. HARDING<sup>1</sup> AND ALEXANDER G. MUSLIMOV<sup>3</sup>

*ApJ Letter, 2000, 531, in press*

### ABSTRACT

We reinvestigate the radio pulsar “death lines” within the framework of two different types of polar cap acceleration models, i.e., the vacuum gap model and the space-charge-limited flow model, with either curvature radiation or inverse Compton scattering photons as the source of pairs. General relativistic frame-dragging is taken into account in both models. We find that the inverse Compton scattering induced space-charge-limited flow model can sustain strong pair production in some long-period pulsars, which allows the newly detected 8.5s pulsar PSR J2144-3933 to be radio loud, without assuming a special neutron star equation-of-state or ad hoc magnetic field configurations.

*Subject headings:* pulsar: general - pulsar: individual: PSR J2144-3933 - radiation mechanism: non-thermal

### 1. INTRODUCTION

Copious pair production in pulsar inner magnetospheres has long been conjectured as an essential condition for the radio emission of pulsars since the pioneering work of Sturrock (1971)<sup>4</sup>. Generally speaking, pair production can create a dense plasma which may allow various coherent instabilities to grow, so as to account for the high brightness temperature observed from the pulsars. The secondary pairs (rather than primary particles) with  $\gamma \sim 10^2 - 10^4$  can produce typical radio-band emission within various models (e.g. Ruderman & Sutherland 1975, hereafter RS75; Melrose 1978; Qiao & Lin 1998). As a consequence, the so-called radio pulsar “death line” is defined as a line in a two-dimensional pulsar parameter phase space ( $P - \dot{P}$  diagram,  $P - B_s$  diagram, or  $P - \Phi$  diagram, where  $P$  is the pulsar period,  $\dot{P}$  the pulsar spin-down rate,  $B_s$  the surface magnetic field, and  $\Phi$  the polar cap potential), which separates the pulsars which can support pair production in their inner magnetospheres from those which cannot (RS75; Arons & Scharlemann 1979, hereafter AS79; Chen & Ruderman 1993, hereafter CR93; Rudak & Ritter 1994; Qiao & Zhang 1996; Björnsson 1996; Weatherall & Eilek 1997; Arons 1998, 2000). Present pulsar death line theories require some degree of anomalous field line configurations (multipole component or offset dipole) to interpret known pulsar data. However, a recently discovered long-period (8.5s) pulsar PSR J2144-3933 (Young, Manchester & Johnston 1999) is clearly located well beyond the conventional death valley (CR93), unless special neutron star equation-of-state or even ad hoc magnetic field configurations are assumed. This challenges the widely accepted belief that pair production is essential for pulsar radio emission. Arons (1999) found that this pulsar is located within the death valley of an inverse Compton controlled space-

charge-limited flow model with frame-dragging included, but some degree of the point dipole offset is needed.

### 2. DEATH LINES IN VARIOUS MODELS

The death line has been defined (e.g. RS75) by the condition that the potential drop across the accelerator ( $\Delta V$ ) required to produce enough pairs per primary to screen out the parallel electric field is larger than the maximum potential drop ( $\Phi_{\max}$ ) available from the pulsar, in which case no secondary pairs would be produced<sup>5</sup>.

It is worth noting that pulsar death lines are actually *model-dependent*. Besides the model-dependent  $\Phi_{\max}$  (see [2] and [7]), the form of  $E_{\parallel}$  within the accelerator (which depends on the boundary conditions and on whether the general relativistic frame-dragging effect is taken into account), the typical energy of the  $\gamma$ -ray photons (which depends on whether their origin is curvature radiation (CR) or inverse Compton scattering (ICS)), and the strength of the perpendicular magnetic field the  $\gamma$ -ray photon encounters (which depends on the field strength and the field line curvature near the neutron star surface) can change  $\Delta V$  considerably and alter the death lines. Furthermore, the obliquity of the pulsar (which changes  $E_{\parallel}$  and  $\Phi_{\max}$ ) and the equation-of-state of the neutron star (which changes the moment of inertia  $I = 10^{45} I_{45}$  and the radius  $R = 10^6 R_6$  of the star) will also influence the location of the death lines. As a result, the phase space for pulsars to die should be a “valley” rather than a single line. CR93 defined a death valley, within the framework of the RS75 vacuum gap model, as the phase space range between the death line of the dipolar field configuration and the death line of some special multipolar field configurations. Here we will also adopt such a death valley, and regard it as also including the scatter of obliquities for different pulsars<sup>6</sup>.

<sup>1</sup>Laboratory of High Energy Astrophysics, NASA/Goddard Space Flight Center, Greenbelt, MD 20771

<sup>2</sup>National Research Council Research Associate Fellow

<sup>3</sup>SM&A Corporation, Space Sciences Division, Upper Marlboro, MD 20774

<sup>4</sup>Although some authors argued that pair production might not be an essential condition for pulsar radio emission (e.g. Weatherall & Eilek 1997), no such pairless radio emission theory is fully constructed.

<sup>5</sup>Note that there are some additional criteria to constrain the death lines for the millisecond pulsars (Rudak & Ritter 1994; Qiao & Zhang 1996; Björnsson 1996) and the pulsars with strong surface magnetic fields (Baring & Harding 1998), and we will not address them in this paper.

<sup>6</sup>Strictly speaking, there could be different death lines for pulsars with different obliquities. The death lines could be quite different for the

Modification of the equation-of-state or of the polar cap radius will also modify the death valleys systematically. The surface magnetic field for the star-centered dipolar configuration is  $B_d = 6.4 \times 10^{19} (P\dot{P})^{1/2} I_{45}^{1/2} R_6^{-3}$  regardless of the internal field geometry (Shapiro & Teukolsky 1983; Usov & Melrose 1995). Thus the only model dependence of the dipolar surface field is the offset of the dipole center from the star center.

Two subgroups of inner gap models were proposed by adopting different boundary conditions. The vacuum-like gap model (V model, RS75) assumes strong binding of ions at the neutron star surface ( $E_{\parallel}(z=0) \neq 0$ ), while the space-charge-limited flow model (SCLF model, AS79) assumes free emission of particles from the surface ( $E_{\parallel}(z=0) = 0$ ). Both of these models were originally proposed by assuming that CR of the primary particles is the main mechanism to create  $\gamma$ -ray seeds to ignite the pair production cascades, and by neglecting general relativistic effects. They were improved later by different authors to include ICS and the inertial frame-dragging effects. The role of frame-dragging in pulsar physics was first explored by Muslimov & Tsygan (1992, hereafter MT92) and updated by Muslimov & Harding (1997, hereafter MH97) and Harding & Muslimov (1998, hereafter HM98) within the framework of the SCLF model. MT92 noted that since stellar rotation actually drags the local inertial frame (LIF) to rotate with an angular velocity  $\Omega_{\text{LIF}} \simeq \Omega_* \kappa_g (R/r)^3$  ( $\Omega_*$  is the angular velocity of the star), the electric field required to bring a charged particle into corotation is weaker than that in the flat spacetime, since such a field only needs to compensate the angular velocity difference between  $\Omega_*$  and  $\Omega_{\text{LIF}}$  rather than the difference of  $\Omega_*$  and the angular velocity at infinity (which is 0). As a result, near the star surface, the Goldreich-Julian density becomes<sup>7</sup>

$$\eta_R \simeq -\frac{(\Omega_* - \Omega_{\text{LIF}}) \cdot \mathbf{B}}{2\pi c\alpha} \simeq -\frac{\Omega_* \cdot \mathbf{B}}{2\pi c\alpha} \left[ 1 - \kappa_g \left( \frac{R}{r} \right)^3 \right], \quad (1)$$

where  $\kappa_g \sim (r_g/R)(I/MR^2) \sim 0.15 - 0.27$  (HM98; we will adopt a typical value of 0.15 hereafter),  $\alpha = (1 - r_g/R)^{1/2} \sim 0.78$  is the redshift factor,  $r_g$  is the gravitational radius, and  $M$  is the mass of the neutron star.

### 2.1. Vacuum gap model (V model)

In principle, pulsar  $E_{\parallel}$  arises from the deviation of the local charge density ( $\eta$ ) from the Goldreich-Julian density ( $\eta_R$ ). If the binding energy of the positive ions is large enough to prevent the ions from thermionic or field emission ejection, a vacuum-like gap (RS75) will form right above the neutron star surface, in which the charge depletion is very large (of the order of  $\eta_R$  itself) so that a very strong  $E_{\parallel}$  is built up right above the surface. This picture was questioned since later calculations showed that the ion binding energy is actually not high enough (for recent reviews, see, e.g. Usov & Melrose 1995). Recent observations indicate that some pulsars may favor the existence of such vacuum gaps (Vivekanand & Joshi 1999; Deshpande & Rankin 1999), and some ideas to solve the binding energy problem have been proposed (e.g. Xu, Qiao & Zhang extreme cases of aligned and orthogonal rotators.

<sup>7</sup>For an explicit expression for  $\eta_R$ , see eqs.[4], [8] and [16] of HM98.

1999). The inclusion of ICS in such a model was carried out by Zhang & Qiao (1996) and Zhang et al. (1997), and the corresponding death line was examined by Qiao & Zhang (1996). The influence of the frame-dragging effect on the model has not been examined before.

The maximum potential available for the V model is just the homopolar generator potential, which is the potential difference between the pole and the edge of the polar cap at the star surface and reads

$$\Phi_{\text{max}}(\text{V}) \simeq (1 - \kappa_g) \frac{B_d R^3 \Omega_*^2}{2c^2} \simeq 5.6 \times 10^{12} (\text{Volts}) B_{d,12} P^{-2} R_6^3. \quad (2)$$

Note frame-dragging modifies the flat spacetime result by a factor of  $\zeta = (1 - \kappa_g) \sim 0.85$ , which arises from  $(\Omega_* - \Omega_{\text{LIF}})$ . The solution of the one-dimensional Poisson's equation (the infinitesimal gap in RS75) then gives  $E_{\parallel}(z) = \zeta(2\Omega_* B/c)(h - z)$  and  $\Delta V = \zeta(\Omega_* B/c)h^2$ , which are essentially RS75's results with the correction factor  $\zeta$ .

The gap height depends on three length scales, i.e.,  $l_{\text{acc}}$ , the acceleration scale before the primary electron or positron achieves a high enough energy  $\gamma_c$ ;  $l_e \sim c[\dot{\gamma}(\gamma_c mc^2)/E_c]^{-1}$ , the mean free path of the electron/positron with  $\gamma_c$  to emit one  $\gamma$ -ray quanta with energy  $E_c$ ; and  $l_{\text{ph}} = \chi \rho(B_{\text{cri}}/B_s)(2mc^2/E_c)$ , the mean free path of the  $\gamma$ -photon before being absorbed, where  $B_{\text{cri}} = m^2 c^3 / \hbar e \simeq 4.4 \times 10^{13} \text{G}$  is the critical magnetic field, and  $\chi \sim 0.1$  is the key parameter to describe  $\gamma - B$  absorption coefficient (Erber 1966). The electron mean free path  $l_e$  should not exceed the gap height  $h = l_{\text{acc}} + l_{\text{ph}}$ . For the V model, one gets  $\gamma_c = 2\zeta(e/mc^2)(\Omega_* B/c)l_{\text{acc}}(h - l_{\text{acc}}/2)$  with the form of  $E_{\parallel}$ . For the CR-induced cascade model, we have  $E_c = (3/2)(\hbar c/\rho)\gamma_c^3$ , and  $l_e = (9/4)(\hbar c/e^2)\rho\gamma_c^{-1} \ll l_{\text{ph}} \sim l_{\text{acc}} \sim h$ . To treat the gap breakdown process, we are actually looking for the minimum of  $h$ , which could be obtained by setting the derivative  $h$  with respect to  $l_{\text{acc}}$  to zero. With some approximations, we finally get the gap parameters as  $h = 5.0 \times 10^3 (\text{cm}) \zeta^{-3/7} P^{3/7} B_{12}^{-4/7} \rho_6^{2/7}$ , and  $\Delta V = 1.6 \times 10^{12} (\text{Volts}) \zeta^{1/7} P^{-1/7} B_{12}^{-1/7} \rho_6^{4/7}$ , which are analogous to RS75 (their eqs.[22],[23] except for the  $\zeta$  correction), who treated the problem by simply adopting  $h \sim l_{\text{ph}}$ . By setting  $\Delta V = \Phi_{\text{max}}(\text{V})$ , we get the death lines of this model ( $\zeta \sim 0.85$  has been adopted) (cf. eqs.[6],[8] of CR93)

$$\log \dot{P} = (11/4) \log P - 14.62 \quad [\text{I}] \quad (3)$$

$$\log \dot{P} = (9/4) \log P - 16.58 + \log \rho_6 \quad [\text{I}'] \quad (4)$$

for the dipolar and the  $\rho \sim R$ ,  $B_s \sim B_d$  multipolar field configuration, respectively.

For the resonant ICS-induced gap, we have  $E_c = 2\gamma\hbar(eB/mc)$  (Zhang et al. 1997; HM98), and  $\dot{\gamma}_{\text{res}} \sim 4.92 \times 10^{11} B_{12}^2 T_6 \gamma_c^{-1}$  (Dermer 1990), so that  $l_e \sim 0.00276 \gamma_c^2 B_{12}^{-1} T_6^{-1}$ . Since  $l_{\text{acc}} \ll l_e \sim l_{\text{ph}}$  for the ICS case, we solve the gap height by setting  $h \sim l_{\text{ph}} \sim l_e$ . Also treating  $T_6$  self-consistently through self-sustained polar cap heating, i.e.,  $T = (e\Delta V \dot{N} / \sigma \pi r_p^2)^{1/4}$ , where  $\dot{N} = (\Omega B / 4\pi e) \pi r_p^2$  is the polar cap luminosity, and  $r_p$

is the polar cap radius, we finally get the gap height  $h = 2.6 \times 10^4 (\text{cm}) P^{1/7} B_{s,12}^{-11/7} \rho_6^{4/7} \zeta^{-1/14}$ , the gap potential  $\Delta V = 4.2 \times 10^{13} (\text{Volts}) P^{-5/7} B_{s,12}^{-15/7} \rho_6^{8/7} \zeta^{6/7}$ , and the surface temperature  $T_6 = 5.9 B_{12}^{-2/7} P^{-3/7} \rho_6^{2/7} \zeta^{3/14}$  (Note that such a high polar cap temperature conflicts with the observations). The death lines of this model are then<sup>8</sup>

$$\log \dot{P} = (2/11) \log P - 13.07 \quad [\text{II}] \quad (5)$$

$$\log \dot{P} = (-2/11) \log P - 14.50 + (8/11) \log \rho_6 \quad [\text{II}'] \quad (6)$$

for dipolar and multipolar configurations, respectively.

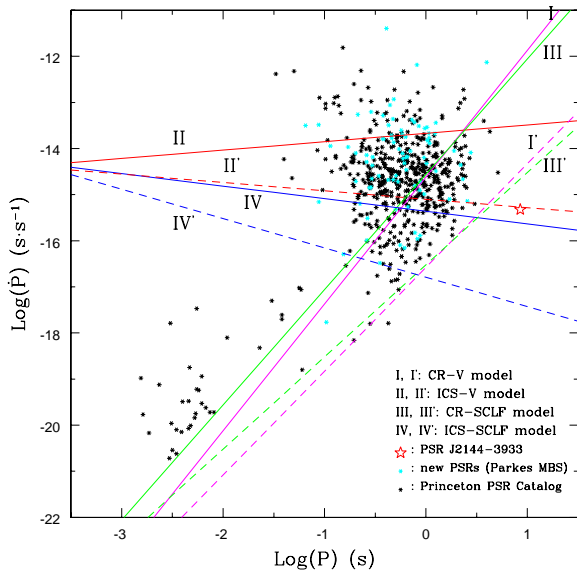


FIG. 1.— Death lines in various models. Solid lines are for dipole, and dashed lines are for  $\rho \sim 10^6 \text{cm}$ ,  $B_s \sim B_d$  multipole. Other captions are marked in the plot. Pulsar data follow the latest results (Manchester et al. 1999).

## 2.2. Space-charge-limited flow model (SCLF model)

If the charged particles (electrons or ions) can actually be pulled out freely from the neutron star surface (which is favored by ion binding energy calculations), a space-charge-limited flow is a natural picture, with  $E_{\parallel} = 0$  at the surface. The  $E_{\parallel}$  at higher altitudes then arises from the small imbalance of the local charge density  $\eta$  from  $\eta_R$  (eq.[1]) due to the flow of the charged particles along field lines. The conservation of current requires  $\eta \propto r^{-3}$ , thus the deviation ( $\eta - \eta_R$ ) arises from the extra  $r$ -dependence of  $\eta_R$  (besides  $B$  declination, which is  $\propto r^{-3}$ ). In flat spacetime, this dependence is just the “flaring” of the field lines, on which the AS79’s pioneering SCLF model is based. Since such a deviation is so small, it takes a long length scale for a particle to be accelerated to pair producing energy via a gradual built-up of  $E_{\parallel}$ , so that the gap shape is usually narrow and long. The maximum potential available in this model is much smaller than the one available in V models (see footnote 9), so that the death

lines in this model are very high (see eq.[48], [50] of AS79). The ICS-induced version of such a SCLF model was presented by Luo (1996). HM98 explicitly studied both CR- and ICS- controlled SCLF accelerators with the frame-dragging effect included, and such a model is very good in interpreting high energy radiation luminosities of the spin-powered pulsars (Zhang & Harding 2000, hereafter ZH00). The inclusion of the general relativistic frame-dragging effect in such SCLF models (MT92; MH97) is essential in two respects. First, besides the  $B$  declination,  $\eta_R$  in curved spacetime has an extra  $(R/r)^3$  dependence (see second term in the bracket of eq.[1]), while the current conservation requirement leads to  $\eta \simeq -\frac{\Omega_* \cdot \mathbf{B}}{2\pi c \alpha} (1 - \kappa_g)$  near the surface. As a result,  $E_{\parallel}$  is built up much faster. Secondly, the maximum potential available is much larger than the flat spacetime value (but smaller than that in V models), which is<sup>9</sup>

$$\Phi_{\text{max}}(\text{SCLF}) \simeq \kappa_g \frac{B_d R^3 \Omega_*^2}{2c^2} \simeq 1.0 \times 10^{12} (\text{Volts}) B_{d,12} P^{-2} R_6^3. \quad (7)$$

As a result, the death lines are considerably lower than the AS79 model.

By introducing an upper  $E_{\parallel} = 0$  boundary at the pair formation front, HM98 have presented the explicit formalism and detailed numerical simulation of  $E_{\parallel}$  within SCLF accelerators. Unfortunately, simple analytic formulae applicable for all the cases are not available. However, we notice that near the death lines, the height of the accelerators ( $h$ ) are all larger than the polar cap radius  $r_{pc} = [\Omega_* R / c f(1)]^{1/2} R$  ( $f(1) \sim 1.4$  is the factor of curved spacetime), and that the  $E_{\parallel}$  in the accelerators has achieved saturation (see ZH00 for discussions of different regimes of acceleration  $E_{\parallel}$  and the criterion to separate the two regimes, their eq.[53]). In such a case, we can adopt the following approximate acceleration picture: near the star surface,  $E_{\parallel}$  grows approximately linearly with respect to the height  $z$  (thus is analogous to V model in this regime) with the form  $E_{\parallel}(1) \simeq [3\kappa_g / (1 - \epsilon)] (\Omega_* B / c) z \simeq 157 B_{12} P^{-1} z$  (eq.A[3] of HM98), where  $\epsilon = r_g / R \sim 0.4$ , and saturates above  $z \sim r_{pc} / 3$  at a value of  $E_{\parallel}(2) \simeq (3\kappa_g / 2) (\Omega_* \cdot \mathbf{B} / c) r_{pc} (r_{pc} / R) (1 - \xi^2) \simeq 3.5 \times 10^3 B_{12} P^{-2} R_6^2$  (eq.[A5] of HM98), where  $f(1) = 1.4$ ,  $\xi = 0.7$  have been adopted. To study the death lines, we assume that the accelerators are located at the surface, though HM98 have argued that accelerators could be  $(0.5 - 1)R$  above the surface in young pulsars due to anisotropy of the upward versus downward ICS. In old pulsars, the returning positron fraction is smaller, and the lower pair formation front may not exist, so that both the CR- and the ICS- induced SCLF accelerators could be formed at the surface.

For the CR-induced model, we again have  $l_e \ll l_{\text{acc}} \sim l_{ph}$ . Since  $h > r_{pc}$  near the death lines (ZH00), we can adopt  $\gamma_c \sim (e/mc^2) E_{\parallel}(2) l_{\text{acc}}$ . Following the same procedure as for the V model, but using  $\Delta V = E_{\parallel}(2)h$  (recall the quadratic form of V model and note the difference), we get  $h = 3.3 \times 10^5 (\text{cm}) P^{3/2} B_{12}^{-1} \rho_6^{1/2} R_6^{-3/2}$  and

<sup>8</sup>The typical ICS photon energy adopted here is the one for resonant scattering. In the cases of high temperatures, the scatterings above the resonance with the photons at Planck’s peak may become important (Zhang et al. 1997), and the death lines could be lower.

<sup>9</sup>For a full expression of  $\Phi_{\text{max}}(\text{SCLF})$ , see eq.[54] of HM98. What we adopted here is the  $\cos \chi$  term, which is much larger than the  $\sin \chi$  term (the maximum available for the AS79 model).

$\Delta V = 3.5 \times 10^{11} (\text{Volts}) P^{-1/2} \rho_6^{1/2} R_6^{1/2}$ . Equating  $\Delta V$  with  $\Phi_{\text{max}}(\text{SCLF})$  (eq.[7]), we get the death lines

$$\log \dot{P} = (5/2) \log P - 14.56 \quad \text{[III]} \quad (8)$$

$$\log \dot{P} = 2 \log P - 16.52 + \log \rho_6 \quad \text{[III]'} \quad (9)$$

for dipolar and multipolar field configurations, respectively.

For the resonant ICS-induced SCLF model, we again have  $l_{\text{acc}} \ll l_e \sim l_{ph}$  and  $h > r_{pc}$ . This brings an important difference with the CR-induced case, that is, one should adopt the linear  $E_{\parallel}$  form, e.g.,  $\gamma_c = (e/mc^2) \int_0^{l_{\text{acc}}} E_{\parallel}(1) dz$  to describe the acceleration phase, but adopt the saturated  $E_{\parallel}$  form to describe the final potential, i.e.,  $\Delta V = E_{\parallel}(2)h$ . Since the SCLF model has a much lower charge deficit than the V model, the number of reversed positrons required to screen the field is only a factor of  $f \simeq |(\partial E_{\parallel}/\partial r)/(8\pi\rho_{GI})|$  of the Goldreich-Julian density (AS79; ZH00), so that one gets less polar cap heating, i.e.,  $T = (e\Delta V \dot{N} f / \sigma\pi r_p^2)^{1/4}$ , in this model. For the saturated accelerators, this factor is roughly  $f \simeq 5.7 \times 10^{-5} P^{-1}$  near the surface (eq.[71] of ZH00). A self consistent treatment of  $T$  finally leads to  $h = 9.7 \times 10^4 (\text{cm}) P^{4/13} B_{12}^{-22/13} \rho_6^{8/13} R_6^{-2/13}$ ,  $\Delta V = 1.0 \times 10^{11} (\text{Volts}) P^{-22/13} B_{12}^{-9/13} \rho_6^{8/13} R_6^{24/13}$ , and  $T_6 = 0.11 P^{-12/13} B_{12}^{1/13} \rho_6^{2/13} R_6^{6/13}$ , so that the death lines are

$$\log \dot{P} = -(3/11) \log P - 15.36 \quad \text{[IV]}(10)$$

$$\log \dot{P} = -(7/11) \log P - 16.79 + (8/11) \log \rho_6. \quad \text{[IV]'}(11)$$

In this model, the polar cap temperature is sustained by the thermal energy released from the crust deposited by the reverse flow of positrons and high energy photons. The primary beam fluctuations (typical timescale  $\sim h/c \sim 3 \times 10^{-6} \text{s}$ ) may result in discontinuous illumination of the polar cap. However, because of the ‘‘inertia’’

of photon diffusion from the relatively deep layers to the photosphere (e.g. Eichler & Cheng 1989), this process is unlikely to affect the average polar cap temperature. For example, it takes  $\sim 6 \times 10^{-3} T_5^{-1.5} \text{s}$  for the photons to diffuse upthrough the surface from a depth of  $100 \text{g cm}^{-2}$ .

### 3. CONCLUSION AND DISCUSSIONS

The death lines of different models are plotted in Fig.1. A remarkable fact is, though PSR J2144-3933 is beyond the death valleys of both the CR- and ICS- induced V models and CR-induced SCLF model, it is well above the *star-centered dipolar* death line of the ICS-induced SCLF model. Thus one does not need to introduce a special neutron star equation-of-state or anomalous field configurations at all to maintain strong pair formation in this pulsar. The ICS-SCLF death lines of Fig.1 imply a very large phase space for radio emission in the long period regime, thought previously to be radio forbidden. In fact, Young et al. (1999) argued that the population of pulsars with parameters similar to PSR J2144-3933 is very large, since the detectability of such pulsars is very small due to their small polar caps. We expect more pulsars to be detected in this region. A general trend in Fig.1 is that death lines in the ICS-induced models have much flatter slopes than those in the CR-induced model. This arises from the very different  $P$ -,  $B_s$ - dependences of both  $l_{ph}$  and  $l_e$  for the resonant ICS processes. The saturation of  $E_{\parallel}$  in long period pulsars is critical in lowering the death lines in the SCLF models relative to those of the V models<sup>10</sup>. The difference is more prominent in ICS- induced models. For the ICS-SCLF model, our death lines are lower than the ones derived in Arons (2000). The difference might be due to the different polar cap temperature treatments.

We thank the referee for good comments and suggestions and Demosthenes Kazanas, G.J.Qiao, R.X.Xu, and Z.Zheng for interesting discussions or helpful comments.

### REFERENCES

- Arons, J. 1998, in: N. Shibazaki et al. (eds), Neutron Stars and Pulsars, (Tokyo: Universal Academy Press, Inc.), 339  
—, 1999, in: M. Kramer et al. (eds), Pulsar Astronomy: 2000 and beyond, IAU Colloq. 177 (Bonn: ASP Conf. Ser.), in press (astro-ph/9911478)  
Arons, J., & Scharlemann, E.T. 1979, ApJ, 231, 854 (AS79)  
Baring, M.G., & Harding, A.K. 1998, ApJ, 507, L55  
Björnsson, C.-I. 1996, ApJ, 471, 321  
Chen, K., & Ruderman, M.A. 1993, ApJ, 402, 264 (CR93)  
Dermer, C.D. 1990, ApJ, 360, 197  
Deshpande, A.A., & Rankin, J.M. 1999, ApJ, 524, 1008  
Eichler, D., & Cheng, A.F. 1989, ApJ, 336, 360  
Erber, T. 1966, Rev. Mod. Phys., 38, 626  
Harding, A.K., & Muslimov, A.G. 1998, ApJ, 508, 328 (HM98)  
Luo, Q. 1996, ApJ, 468, 338  
Manchester, R.N., et al. 1999, in: M. Kramer et al. (eds), Pulsar Astronomy: 2000 and beyond, IAU Colloq. 177 (Bonn: ASP Conf. Ser.), in press (astro-ph/9911319)  
Melrose, D. 1978, ApJ, 225, 557  
Muslimov, A.G., & Harding, A.K. 1997, ApJ, 485, 735 (MH97)  
Muslimov, A.G., & Tsygan, A.I. 1992, MNRAS, 255, 61 (MT92)  
Qiao, G.J., & Lin, W.P. 1998, A&A, 333, 172  
Qiao, G.J., & Zhang, B. 1996, A&A, 306, L5  
Rudak, B., & Ritter, H. 1994, MNRAS, 267, 513  
Ruderman, M.A., & Sutherland, P.G. 1975, ApJ, 196, 51 (RS75)  
Shapiro, S.L., & Teukolsky, S.A. 1983, Black Holes, White Dwarfs, and Neutron Stars: The Physics of Compact Objects (New York: Wiley)  
Sturrock, P.A. 1971, ApJ, 164, 529  
Usov, V.V., & Melrose, D.B. 1995, Australian J. Phys., 48, 571  
Vivekanand, M., & Joshi, B.C. 1999, ApJ, 515, 398  
Weatherall, J.C., & Eilek, J.A. 1997, ApJ, 474, 407  
Xu, R.X., Qiao, G.J., & Zhang, B. 1999, ApJ, 522, L109  
Young, M.D., Manchester, R.N., & Johnston, S. 1999, Nature, 400, 848  
Zhang, B., & Harding, A.K. 2000, ApJ, 532, in press (astro-ph/9911028) (ZH00)  
Zhang, B., Qiao, G.J. 1996, A&A, 310, 135  
Zhang, B., Qiao, G.J., Lin, W.P., & Han, J.L. 1997, ApJ, 478, 313

<sup>10</sup>V models also have  $E_{\parallel}$  saturation, but only near the death lines when  $h \sim r_{pc}$  (RS75). SCLF models, however, can have  $E_{\parallel}$  saturation much farther away from the death lines and thus allows a greater distance for pair production before  $\Phi_{\text{max}}$  is reached.